

**Magnetic field resistant quantum interferences in Josephson junctions based on bismuth nanowires**Chuan Li,<sup>1</sup> A. Kasumov,<sup>1,5</sup> Anil Murani,<sup>1</sup> Shamashis Sengupta,<sup>2</sup> F. Fortuna,<sup>2</sup> K. Napolskii,<sup>3,4</sup> D. Koshkodaev,<sup>4</sup> G. Tsirlina,<sup>3</sup> Y. Kasumov,<sup>5</sup> I. Khodos,<sup>5</sup> R. Deblock,<sup>1</sup> M. Ferrier,<sup>1</sup> S. Guéron,<sup>1</sup> and H. Bouchiat<sup>1</sup><sup>1</sup>*LPS, Univ. Paris-Sud, CNRS, UMR 8502, F-91405 Orsay Cedex, France*<sup>2</sup>*CSNSM, University Paris-Sud, IN2P3, UMR 8609, F-91405 Orsay Cedex, France*<sup>3</sup>*Faculty of Chemistry, Moscow State University, Leninskie Gory, 1-building 3, Moscow, 119991, Russia*<sup>4</sup>*Department of Material Sciences, Moscow State University, Leninskie Gory, Moscow, 119991, Russia*<sup>5</sup>*Institute of Microelectronics Technology and High Purity Materials, RAS, ac. Ossipyan, 6, Chernogolovka, Moscow Region, 142432, Russia*

(Received 13 June 2014; revised manuscript received 28 November 2014; published 23 December 2014)

We investigate proximity-induced superconductivity in micrometer-long bismuth nanowires connected to superconducting electrodes with a high critical field. At low temperature we measure a supercurrent that persists in magnetic fields as high as the critical field of the electrodes (above 11 T). The critical current is also strongly modulated by the magnetic field. In certain samples we find regular, rapid SQUID-like periodic oscillations occurring up to high fields. Other samples exhibit less periodic but full modulations of the critical current on Tesla field scales, with field-caused extinctions of the supercurrent. These findings indicate the existence of low dimensionality, phase coherent, interfering conducting regions through the samples, with a subtle interplay between orbital and spin contributions. We relate these surprising results to the electronic properties of the surface states of bismuth, strong Rashba spin-orbit coupling, large effective  $g$  factors, and their effect on the induced pair correlations. In particular, we emphasize the possible contribution of topological edge states of specific facets of the nanowires.

DOI: [10.1103/PhysRevB.90.245427](https://doi.org/10.1103/PhysRevB.90.245427)

PACS number(s): 73.63.-b, 74.45.+c, 74.78.Na

In the superconducting proximity effect, singlet pair correlations can penetrate quite far into a nonsuperconducting (normal,  $N$ ) conductor. This penetration, which can lead to supercurrents through normal conductors several micrometers long connected to two superconductors ( $S$ ), results from quantum interference between all conduction channels in the  $N$ . In a microscopic picture, the supercurrent is carried by Andreev states, combinations of time-reversed electron and hole wavefunctions confined to the  $N$ . It is thus natural to consider that this interference is destroyed not only by inelastic scattering, but also by time-reversal symmetry breaking. Indeed, a magnetic field is known to suppress the supercurrent via both orbital (Aharonov Bohm phase accumulation) and spin (Zeeman dephasing) effects. Nevertheless, supercurrents have been induced through ferromagnets ( $F$ ). The oscillatory sign and decaying intensity of the supercurrent with increasing  $F$  thickness illustrate the dephasing role played by the exchange field. Time-reversal invariant spin orbit interactions offer new possibilities: they correlate the spatial and spin components of the induced Andreev pairs, leading to coupling between singlet and triplet pairing [1,2], arbitrary Josephson phase shifts in an exchange or Zeeman field ( $\phi$  junction behavior) [3–5], and the possible formation of Majorana fermions at the interface between semiconducting nanowires and superconductors [6].

In this paper, we probe the superconducting proximity effect in crystalline bismuth nanowires, a system with extremely high Rashba spin-orbit coupling (SOC), connected to superconducting electrodes with standard  $s$ -wave pairing and a very high critical field  $H_c$ . The complex interference pattern we measure, up to fields such that the Zeeman energy  $E_Z$  reaches the spin-orbit and Fermi energies ( $E_F$ ), uniquely reveals the role played by both spin and orbital degrees of freedom.

Bismuth is a semimetal with rhombohedral structure whose bulk Fermi surface is strongly anisotropic. Bi's strong atomic SOC leads to extremely high and anisotropic effective  $g$  factors

( $g_{\text{eff}} \sim 100$ ). The semimetallic character leads to unusually large Fermi wavelengths,  $\lambda_F \sim 50$  nm [7]. Therefore, in nanostructures only a few  $\lambda_F$  thick or wide, because of quantum confinement, the surface states rather than the bulk states should play a major role [8,9]. Angle-resolved photoemission (ARPES) revealed such electronic surface states with almost free electronic mass and nanometer-size  $\lambda_F$ . Those states are remarkable in that the energy bands display a huge Rashba spin splitting, due to inversion-symmetry breaking at the surface combined with Bi's high atomic SOC. ARPES of differently oriented Bi surfaces [10] and spin resolved ARPES [11] find spin splitting energies around 0.1 eV, as high as  $E_F$ . The (111) surface, perpendicular to the rhombohedral axis, is particular because it possesses states on the top bilayer that are decoupled from the bulk. Moreover, one-dimensional (1D) quantum spin Hall states have been predicted at the edge of these (111) surfaces [12]. Quite recently, scanning tunneling microscopy have indeed found 1D edge states around single crystalline bilayer islands atop BiSe and bulk Bi(111) crystals [13,14]. 1D topological states of (114) surfaces have also been seen by ARPES [15]. Thus 100-nm-wide Bi nanowires seem ideal to investigate the effect of SOC on the superconducting proximity effect, in the regime barely explored of a carrier spin-splitting energy comparable to  $E_F$ . In addition, the surface states' relatively high  $g_{\text{eff}}$  (between 10 and 100, depending on the field direction) [16], imply that  $E_Z$  can reach  $E_F$  and spin-splitting energy at fields of about 10 T. Finally, the relative orientation of Zeeman and orbital fields can be varied, leading to even richer physics.

In the following, we present experiments on Bi nanowires connected to high  $H_c$  superconductors that show striking differences with ordinary Josephson SNS junctions: the supercurrent persists up to fields as high as 10 T. In some cases the field enhances the critical current  $I_c$ . We also find oscillations of  $I_c$ : some samples display SQUID-like oscillations with a

period in the hundred-Gauss range, and a higher, Tesla range, modulation; others display only a high field modulation of  $I_c$ , with complete extinctions at specific fields. We show that these observations are well explained by interfering Andreev pairs confined to a small number of 1D conducting regions, possibly topological edge states of specific facets of the nanowires. A subtle interplay between orbital and spin contributions explains the amplitude and period of interferences.

The Bi nanowires are electrochemically grown in the 90 ± 10-nm-wide pores of a polycarbonate track-etched membrane and released by dissolution of the membrane (see Supplemental Material [17]). X-ray diffraction and transmission electron microscopy demonstrate the high crystallinity of the few-micrometer-long nanowires, with no high-angle grain boundaries. A 10- to 20-nm-thick external organic amorphous layer is also found, probably a protective residual polycarbonate coating. Given the nanometer-size  $\lambda_F$  of Bi's surface states [7], more than 100 conduction channels are expected at the wire surface if considered a homogeneous cylinder. The nanowires are, however, actually faceted polyhedra, each facet having a potentially different crystalline orientation. Thus, some facets can be insulating [18] while others, such as (111) or (114), may have 1D topological edge states. The nanowires are deposited onto an oxidized Si substrate with prepatterned electrodes. The superconducting contacts to the Bi nanowires, and connection to the electrodes, are realized in a dual electron and ion beam microscope equipped with a gas injection system. The focused Ga ion beam (FIB) decomposes a tungsten carbonyl vapor, producing a carbon and gallium-doped amorphous tungsten wire roughly 100 nm thick and wide. The superconductive properties of these  $W$  wires are impressive, with a transition temperature  $T_c \sim 4$  K,  $I_c \sim 100 \mu\text{A}$ , and  $H_c$  above 11 T at low temperature (LT) [19,20]. The superconducting gap measured by scanning tunneling spectroscopy [21] is  $\Delta_W = 0.8$  meV. We have checked that SNS junctions with micrometer-long Au wires contacted to such  $W$  wires behave similarly to more conventionally fabricated SNS junctions [22]. Because the FIB is used to cut the end of the polycarbonate-coated Bi wire before  $W$  deposition, a good, albeit not perfect, transparency can be achieved. The rest of the wire remains coated with polycarbonate. To minimize ion damage, both cutting and deposition are performed with an ion current below 10 pA. The contacts degrade with time, so the samples were cooled within hours after their connection, except for Bi3 (see below), which was kept several weeks in a vacuum at room temperature (RT) after the first set of measurements, and whose resistance doubled.

We have investigated the LT resistance of ten samples. Below the  $T_c$  of the  $W$  electrodes, the resistance is mostly due to the two probe resistance of the Bi nanowires. Although the wires have similar dimensions, this resistance varies widely, between 1 and 30 k $\Omega$ . Since the intrinsic resistance of the Bi wires is only expected to be a few hundred  $\Omega$  (if one extrapolates reports on much longer wires of similar diameters [8]), this indicates that the wire-contact interface resistance dominates.

Proximity-induced superconductivity causes a resistance decrease below the  $W$ 's  $T_c$  in five samples out of ten. A supercurrent, corresponding to a zero-resistance state, is detectable in three samples. Two other samples display an

incomplete proximity effect: the resistance drop is small (3–10%), and turns into a resistance increase (of about 10%) as  $T$  is lowered further. The LT differential resistance of those two samples is peaked at low current, due to the interplay of interactions and a low transparency of the Bi- $W$  interface [23]. These results imply that our Bi nanowires are not *intrinsically* superconducting, in contrast to the superconductivity below 1 K found in prior work [24]. Those latter nanowires were unprotected against oxidation, resulting in more pronounced surface disorder than ours. Kobayashi *et al.* [25] also found intrinsic superconductivity with  $T_c = 8$  K and  $H_c = 4$  T in highly disordered nanowires with nanometer-size grains, but no intrinsic superconductivity down to 0.5 K in oxide-free crystalline Bi nanowires. There is, however, one report of intrinsic superconductivity in arrays of single-crystal Bi nanowires grown, as ours, in polycarbonate membranes (but with a different electrolyte) [26], with  $T_c \sim 0.64$  K and  $H_c$  smaller than 0.5 T.

In the following, we focus on the three samples with a detectable supercurrent, Bi<sub>1</sub>, Bi<sub>2</sub>, and Bi<sub>3</sub>, which are all 2  $\mu\text{m}$  long. The normal state resistances,  $R_N$ , measured below the  $W$ 's  $T_c$ , are, respectively, 1, 13, and 16 k $\Omega$ . We also present successive cool downs of Bi<sub>3</sub>, with changed orientations between wire and field. The sample is called Bi<sub>3</sub><sup>\*</sup>, since its RT resistance increased to 27 k $\Omega$ , implying a worsening of the contact to the  $W$  electrodes. The zero bias resistance drops to zero below 0.8 K, and the differential resistance is zero below a switching current of 1.5, 0.1, and 0.075  $\mu\text{A}$  for Bi<sub>1</sub>, Bi<sub>2</sub>, and Bi<sub>3</sub>, respectively, in zero field and at 100 mK. In the following, we equate this switching current and  $I_c$ . We also extrapolate  $I_c = 30$  nA for Bi<sub>3</sub><sup>\*</sup>, even though it does not display a fully zero-resistance state. The  $R_N I_c$  product ranges between 0.75 and 1.5 meV, the same order of magnitude as  $\Delta_W$  [27]. This is typical of short Josephson SNS junctions and implies that  $\Delta_W$  is less than 10 times the Thouless energy  $\hbar D/L^2 \sim \hbar v_F l_e/L^2$  [28]. A Fermi velocity  $v_F \leq 310^5$  m/s yields a mean free path  $l_e \simeq 2 \mu\text{m} \simeq L$ , confirming the ballistic nature of transport of Andreev pairs. The temperature dependence of Bi<sub>3</sub>'s differential resistance, and Shapiro steps under irradiation at frequency  $f$ , that appear at the expected dc voltages  $2eV_n = nhf$ , are shown in the Supplemental Materials [17].

The most striking result is the magnetic field dependence of  $I_c$  (Figs. 1 and 2, field perpendicular to the wires, and Fig. 3 with three different orientations). First, the supercurrent persists up to very high fields: higher than 6 T for Bi<sub>1</sub> and Bi<sub>2</sub>, and 11 T for Bi<sub>3</sub>: those values are merely limited by the fields achievable in the experiments. Second,  $I_c$  of all three samples is strongly modulated by the field: two samples, Bi<sub>1</sub> and Bi<sub>3</sub>, display SQUID-like oscillations of  $I_c$ , with a period of 800 G for Bi<sub>1</sub> and 140 G for Bi<sub>3</sub>. These rapid oscillations persist to high fields, up to 10 T for Bi<sub>3</sub> (not shown) [29]. The critical current of Bi<sub>3</sub> is also modulated with a second period of about 0.3 T. Finally,  $I_c$  is also modulated aperiodically on the Tesla scale for Bi<sub>1</sub>, Bi<sub>2</sub>, and Bi<sub>3</sub><sup>\*</sup>.

In samples without rapid SQUID-like oscillations, the high field modulation causes a full extinction of the supercurrent in Bi<sub>2</sub> and Bi<sub>3</sub><sup>\*</sup>, with entire field intervals having zero supercurrent and finite resistance. We explored three perpendicular field orientations for Bi<sub>3</sub><sup>\*</sup>, including one along the wire axis (Fig. 3).

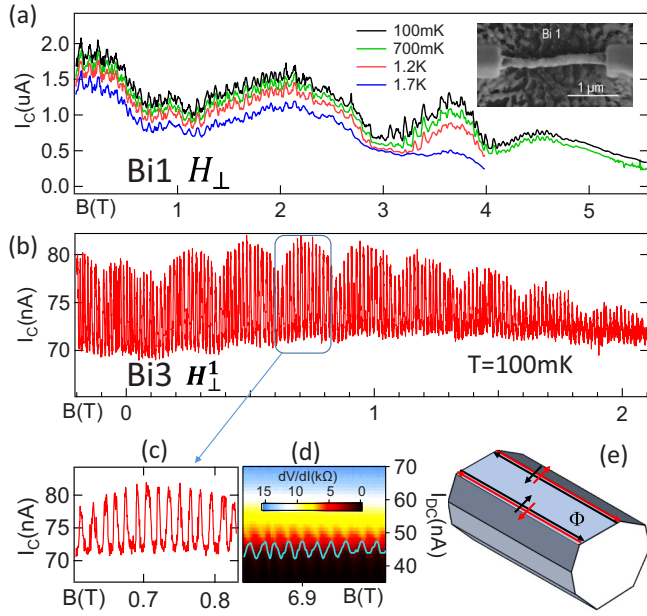


FIG. 1. (Color online) Magnetic-field dependence of the supercurrent of Bi<sub>1</sub> (a) and Bi<sub>3</sub> (b–d), in a perpendicular field. Fast, squid-like oscillations with periods of 800 and 150 G for Bi<sub>1</sub> and Bi<sub>3</sub>, respectively, are noticeable, up to unusually high fields (at least 6 T for Bi<sub>1</sub>, 10 T for Bi<sub>3</sub>). Bi<sub>3</sub> displays an additional periodic modulation with a 2300 G period, and an irregular modulation of Bi<sub>1</sub>'s critical current occurs on the Tesla scale. (e) Sketch of two edge states interfering to produce SQUID-like oscillations up to high field. Inset: Scanning electron micrograph of Bi<sub>1</sub> and its superconducting contacts.

The field modulation patterns of  $I_c$  differ. High resistance peaks occur at different fields (8, 9, and 5 T). The small-period, SQUID-like oscillations of the first cool down are not detectable in these subsequent cool downs.

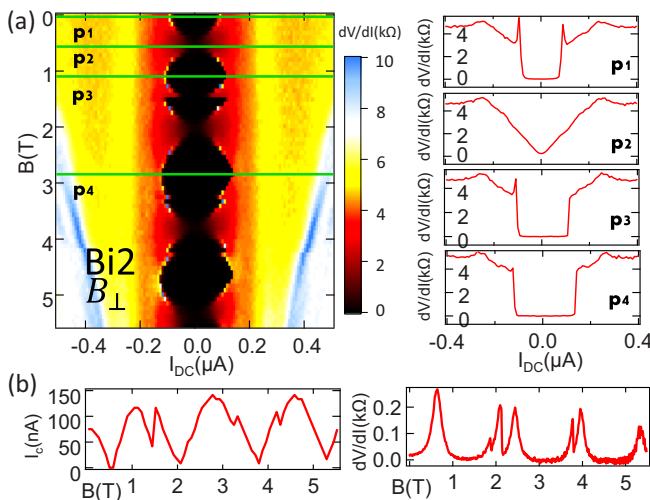


FIG. 2. (Color online) (a) Color-coded differential resistance of Bi<sub>2</sub>, as a function of dc current and magnetic field, with selected differential resistance curves on the right. (b and c) Field dependence of  $I_c$  and zero bias differential resistance extracted from panel (a). Note the oscillatory behavior on the Tesla scale, and the increase of maximal critical current with field.

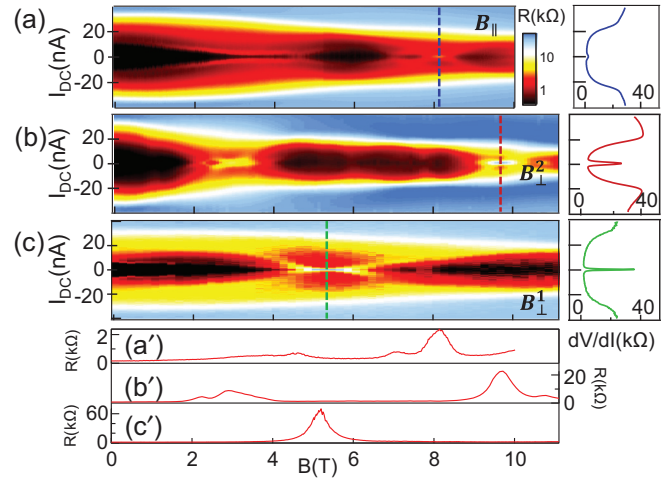


FIG. 3. (Color online) Color-coded differential resistance as a function of current and field, and extracted curves, for three field orientations, on sample Bi<sub>3</sub>\* (that corresponds to sample Bi<sub>3</sub> after thermal cycling and aging). (a) Field along the nanowire axis; (b, c) two field orientations perpendicular to the wire axis.

We now discuss these interference patterns by considering field-induced phase shifts of the Andreev pairs wave functions, via orbital or spin effects. We first recall the generic field dependence of  $I_c$  of ordinary SNS junctions with many conduction channels. The magnetic field suppresses  $I_c$  via two different pair-breaking mechanisms. In the semiclassical limit ( $\lambda_F$  much smaller than all sample dimensions), orbital phase breaking is due to the Aharonov-Bohm phase difference between different Andreev pairs that follow different trajectories through the  $N$ . This orbital dephasing suppresses the supercurrent at fields corresponding to a flux quantum through the sample, as observed experimentally, e.g., in Au wires [22]. In samples with a very small area perpendicular to the magnetic field, this orbital dephasing is weak, and the spin phase breaking caused by the Zeeman effect becomes noticeable. The Zeeman effect causes a phase difference between the electron and hole components of a given Andreev pair, given by  $E_Z \tau / \hbar$  on a trajectory of length  $L_i$  ( $\tau = L_i / v_F$  is the time to cross the sample). Summing the contributions of all Andreev pairs trajectories, when the number of channels is large, yields an exponential supercurrent suppression with magnetic field.

All three Bi wires have an area perpendicular to the field of  $2 \mu\text{m}$  by  $100 \text{ nm}$ , so that one flux quantum corresponds to 50 G, three orders of magnitude smaller than the supercurrent extinction field found in the experiment. The persistence of supercurrents to fields as high as 10 T must, therefore, be due to very few, quasiballistic, 1D channels whose width does not exceed  $\lambda_F$ . These channels could be along the edges of particular facets parallel to the nanowire axis [30]. The small period (few 100 G), SQUID-like oscillations of  $I_c$  in Bi<sub>1</sub> and Bi<sub>3</sub>, are then the manifestation of quantum interference between Andreev pairs belonging to two such 1D edge channels. Such edge states could be those of the (111) or (114) surfaces, or of others possessing similar topological properties. Since the period of the oscillation corresponds to the flux enclosed between the interfering channels, the measured periods of 140 G for Bi<sub>3</sub> and 800 G for Bi<sub>1</sub> would

correspond to 1D channels parallel to the wire axis, distant by 70 and 12 nm, respectively, fully consistent with typical facet widths. This interference pattern recalls the periodic oscillations of the Josephson current carried by spin Hall edge states observed in a 2D topological insulator connected to superconducting electrodes [31]. Note that “ordinary” diffusive facets in parallel with these 1D ballistic channels may exist, but their contribution to the supercurrent should be small at zero field and vanish at fields above 50 G (one  $\Phi_0$  through the sample).

We now discuss the supercurrent modulation at higher field and argue that it is due to the difference between the electron and hole wavevectors of the Andreev pairs. The magnetic field, via  $E_Z$ , shifts the wavevectors of carriers of opposite spin at the Fermi level [4,5]. Within linear approximation, the phase difference accumulated between the electron and hole components of opposite spin along a 1D ballistic trajectory of length  $L$  is [3,32]  $\delta\phi(B) = E_Z L / (\hbar v_F) = g_{\text{eff}} \mu_B B_{\parallel} (\hbar v_F / L)$ , with  $B_{\parallel}$  the field component along the spin-orbit field. (Note, the exact similarity to 1D ballistic superconducting-ferromagnetic-superconducting (SFS) junctions [33]). Taking as parameters typical values of surface states ( $v_F \simeq 3 \cdot 10^5$  m/s and  $g_{\text{eff}} = 30$ ) yields a characteristic modulation period in the Tesla range, so that we believe that the large field modulation of  $I_c$  seen on all samples is due to this spin-dephasing effect. The difference in interference pattern of the various samples, as well as for the three field orientations of  $\text{Bi}_3^*$ , is expected, given the anisotropy of the Bi facets and the corresponding different  $g_{\text{eff}}$ , which can vary by more than an order of magnitude. It is easy to reproduce the experimental data on  $\text{Bi}_3$  by considering the interference between two channels of transmissions differing by a factor 8, enclosing a surface of the order of the sample area. One has to take  $g_{\text{eff}} \sim 100$  for the weakly transmitting channel, yielding an amplitude modulation of the small-period orbital SQUID-like oscillations with a 0.3 T period, and a much smaller  $g_{\text{eff}}$  for the strongly transmitting channel [34].

In this picture, the full extinction of the supercurrent at nearly periodic field values is attributed to the Zeeman-induced

$(2n + 1)\pi$  phase differences (with  $n$  integer) between the electron and hole components of the supercurrent-carrying Andreev pairs. Such full extinction (complete destructive interference) is thus restricted to a single current-carrying channel. This seems to be the case in  $\text{Bi}_2$  and  $\text{Bi}_3^*$ , since they do not display SQUID-like oscillations (that require two channels). The  $\text{Bi}_3^*$  behavior is especially dramatic around 5 T [Figs. 3(c) and 3(c')], with a zero-bias resistance that peaks at a value even higher than the normal state resistance. Such a zero-bias resistance peak is typical of a current-biased superconducting tunnel junction with zero supercurrent. A final important finding is the enhancement of  $I_c$  by the magnetic field.  $\text{Bi}_2$ 's critical current at 5 T is twice that of zero field [Figs. 2(a) and 2(b)]. A similar but smaller increase between 0 and 0.75 T is also seen in  $\text{Bi}_3$  [Fig. 1(b)]. This increase of  $I_c$  with field may be attributable to the strong SOC, as predicted in  $\phi$  junctions [3,34].

In conclusion, we have shown evidence of quantum interference in Bi nanowires-based Josephson junctions, which persist up to very high magnetic fields. The period and decay scales of the oscillations of critical current reveal the physical mechanism at their origin: the interferences occur between strongly confined 1D channels, possibly located at the edges of specific facets of the wires. The physical origin of this confinement could be the topological nature of these particular facets. This confinement may also be favored in the superconducting state by the high magnetic field, which is known to induce inhomogeneous superconductivity in 2D superconductors with large Rashba SOC [35].

We acknowledge fruitful discussions with Alexei Chepelianskii, Michael Feigelman, Pavel Ioselevich, Pascal Simon, Sacha Buzdin, and Sergey Mironov. This work is supported by a Franco-Russian RFBR Grant No. 13-02-91058-CNRS. The LPS group benefits from financial support from CNRS and of the French National Research Agency (ANR SUPERGRAPH-SIMI-10-LS-100617-12-01 and Grant No. ANR-12-BJ04-0016-MASH). MSU group is partly supported by RFBR Grant No. 13-03-01089.

- 
- [1] Lev P. Gor'kov and Emmanuel I. Rashba, *Phys. Rev. Lett.* **87**, 037004 (2001).
  - [2] F. S. Bergeret, A. F. Volkov, and K. B. Efetov, *Rev. Mod. Phys.* **77**, 1321 (2005).
  - [3] A. Buzdin, *Phys. Rev. Lett.* **101**, 107005 (2008).
  - [4] A. A. Reynoso, G. Usaj, C. A. Balseiro, D. Feinberg, and M. Avignon, *Phys. Rev. B* **86**, 214519 (2012).
  - [5] Tomohiro Yokoyama, Mikio Eto, Yuli V. Nazarov, *Phys. Rev. B* **89**, 195407 (2014).
  - [6] R. M. Lutchyn, J. D. Sau, and S. Das Sarma, *Phys. Rev. Lett.* **105**, 077001 (2010); Y. Oreg, G. Refael, and F. von Oppen, *ibid.* **105**, 177002 (2010); V. Mourik, K. Zuo, S. M. Frolov, S. R. Plissard, E. P. A. M. Bakker and L. P. Kouwenhoven, *Science* **336**, 1003 (2012).
  - [7] P. Hoffman, *Prog. Surf. Sci.* **81** 191 (2006).
  - [8] A. Nikolaeva, D. Gitsu, L. Konopko, M. J. Graf, and T. E. Huber, *Phys. Rev. B* **77**, 075332 (2008).
  - [9] Wei Ning, Fengyu Kong, Chuanying Xi, David Graf, Haifeng Du, Yuyan Han, Jiyong Yang, Mingliang Tian, and Yuheng Zhang, *ACS Nano* **8**, 7506 (2014).
  - [10] Yu. M. Koroteev, G. Bihlmayer, J. E. Gayone, E. V. Chulkov, S. Blügel, P. M. Echenique, and Ph. Hofmann, *Phys. Rev. Lett.* **93**, 046403 (2004).
  - [11] T. Hirahara *et al.*, *Phys. Rev. B* **76**, 153305 (2007).
  - [12] S. Murakami, *Phys. Rev. Lett.* **97**, 236805 (2006).
  - [13] Fang Yang, Lin Miao, Z. F. Wang, Meng-Yu Yao, Fengfeng Zhu, Y. R. Song, Mei-Xiao Wang, Jin-Peng Xu, Alexei V. Fedorov, Z. Sun, G. B. Zhang, Canhua Liu, Feng Liu, Dong Qian, C. L. Gao, and Jin-Feng Jia, *Phys. Rev. Lett.* **109**, 016801 (2012).

- [14] Ilya K. Drozdov, A. Alexandradinata, Sangjun Jeon, Stevan Nadj-Perge, Huiwen Ji, R. J. Cava, B. A. Bernevig, Ali Yazdani, *Nature Phys.* **10**, 664 (2014).
- [15] J. W. Wells, J. H. Dil, F. Meier, J. Lobo-Checa, V. N. Petrov, J. Osterwalder, M. M. Ugeda, I. Fernandez-Torrente, J. I. Pascual, E. D. L. Rienks, M. F. Jensen, and Ph. Hofmann, *Phys. Rev. Lett.* **102**, 096802 (2009).
- [16] B. Seradjeh, J. Wu, and P. Phillips, *Phys. Rev. Lett.* **103**, 136803 (2009).
- [17] See Supplemental Material at <http://link.aps.org/supplemental/10.1103/PhysRevB.90.245427> for more on the electrochemical growth and release of Bi nanowires.
- [18] M. Wada, S. Murakami, F. Freimuth, and G. Bihlmayer, *Phys. Rev. B* **83**, 121310 (2011).
- [19] A. Yu. Kasumov, K. Tsukagoshi, M. Kawamura, T. Kobayashi, Y. Aoyagi, K. Senba, T. Kodama, H. Nishikawa, I. Ikemoto, K. Kikuchi, V. T. Volkov, Yu. A. Kasumov, R. Deblock, S. Guéron, and H. Bouchiat, *Phys. Rev. B* **72**, 033414 (2005).
- [20] J. Wang, C. Shi, M. Tian, Q. Zhang, N. Kumar, J. K. Jain, T. E. Mallouk, and M. H. W. Chan, *Phys. Rev. Lett.* **102**, 247003 (2009); J. Wang, M. Singh, M. Tian, N. Kumar, B. Liu, C. Shi, J. K. Jain, N. Samarth, T. E. Mallouk, and M. H. W. Chan, *Nat. Phys.* **6**, 389 (2010).
- [21] I. Guillamon *et al.*, *New J. Phys.* **10**, 093005 (2008).
- [22] F. Chiodi, M. Ferrier, S. Guéron, J. C. Cuevas, G. Montambaux, F. Fortuna, A. Kasumov, and H. Bouchiat, *Phys. Rev. B* **86**, 064510 (2012).
- [23] H. T. Man, T. M. Klapwijk and A. F. Morpurgo, [arXiv:cond-mat/0504566v1](https://arxiv.org/abs/cond-mat/0504566v1).
- [24] M. Tian, J. Wang, Q. Zhang, N. Kumar, T. E. Mallouk, and M. H. W. Chan, *Nano Lett.* **9**, 3196 (2009).
- [25] M. Tian, J. Wang, N. Kumar, T. Han, Y. Kobayashi, Y. Liu, T. E. Mallouk, and M. H. W. Chan, *Nano Lett.* **6**, 2773 (2006).
- [26] Z. Ye, H. Zhang, H. Liu, W. Wu and Z. Luo, *Nanotechnology* **19**, 085709 (2008).
- [27] A. A. Golubov, M. Yu. Kupriyanov, and E. Iliichev, *Rev. Mod. Phys.* **76**, 411 (2004).
- [28] P. Dubos, H. Courtois, B. Pannetier, F. K. Wilhelm, A. D. Zaikin, and G. Schon, *Phys. Rev. B* **63**, 064502 (2001).
- [29] Periodic magnetoresistance oscillations were observed in BiSe nanowires connected to W. electrodes [D. Zhang, J. Wang, A. M. DaSilva, J. S. Lee, H. R. Gutierrez, M. H. W. Chan, J. Jain, and N. Samarth, *Phys. Rev. B* **84**, 165120 (2011)]. These observations differ from ours, which concern the critical current.
- [30] An alternative hypothesis could be that the nanowires behave as nearly perfect ballistic cylinders, with a quasifull cancelation of the flux of a perpendicular magnetic field. But we doubt this ideal picture can realistically describe our samples.
- [31] S. Hart, H. Ren, T. Wagner, P. Leubner, M. Mühlbauer, C. Brüne, H. Buhmann, L. W. Molenkamp, and A. Yacoby, *Nature Phys.* **10**, 638 (2014).
- [32] P. Ioselevich and M. Feigelman (unpublished).
- [33] A. I. Buzdin, *Rev. Mod. Phys.* **77**, 935 (2005).
- [34] S. V. Mironov, A. S. Mel'nikov, and A. I. Buzdin, [arXiv:1411.1626](https://arxiv.org/abs/1411.1626).
- [35] V. Barzykin and L. P. Gorkov, *Phys. Rev. Lett.* **89**, 227002 (2002); O. V. Dimitrova and M. V. Feigelman, *JETP Lett.* **78**, 637 (2003).